Anais da Academia Brasileira de Ciências (2010) 82(1): 145-151
(Annals of the Brazilian Academy of Sciences)
ISSN 0001-3765
www.scielo.br/aabc

Biaxial testing of canine annulus fibrosus tissue under changing salt concentrations

JACQUES M. HUYGHE

Department of Biomedical Engineering, Engineering Mechanics Institute,
Eindhoven University of Technology, P.O. Box 513, 5600MB Eindhoven, The Netherlands

Manuscript received on July 3, 2008; accepted for publication on February 2, 2009

ABSTRACT

The *in vivo* mechanics of the annulus fibrosus of the intervertebral disc is one of biaxial rather than uniaxial loading. The material properties of the annulus are intimately linked to the osmolarity in the tissue. This paper presents biaxial relaxation experiments of canine annulus fibrosus tissue under stepwise changes of external salt concentration. The force tracings show that stresses are strongly dependent on time, salt concentration and orientation. The force tracing signature of a response to a change in strain, is one of a jump in stress that relaxes partly as the new strain is maintained. The force tracing signature of a stepwise change in salt concentration is a progressive monotonous change in stress towards a new equilibrium value. Although the number of samples does not allow any definitive quantitative conclusions, the trends may shed light on the complex interaction among the directionality of forces, strains and fiber orientation on one hand, and on the other hand, the osmolarity of the tissue. The dual response to a change in strain is understood as an immediate response before fluid flows in or out of the tissue, followed by a progressive readjustment of the fluid content in time because of the gradient in fluid chemical potential between the tissue and the surrounding solution.

Key words: swelling, collagen, osmosis, Donnan, cartilaginous.

INTRODUCTION

Intervertebral disc tissue is a very deformable molecular mixture of an ionized solid and an ionised fluid. It is composed of a gelly-like core, the nucleus pulposus, enclosed within a fibrous ring, the annulus fibrosus. Both are composed of a crosslinked collagen network embedded into a gel of hydrated proteoglycans, in different ratios. The swelling of the tissue is primarily generated by the ionized proteoglycans. Though, it is estimated that 20% of the water is absorbed by the collagen network. Different modelling strategies have been proposed to grasp its coupled electro-chemo-mechanical properties (Huyghe 1999, Iatridis et al. 2003, van Loon et al. 2003, Huyghe et al. 2003, Schroeder et al. 2006, Schroeder et al. 2008). The constitutive relationships of an intervertebral disc tissue are subdivided into 2 categories (Huyghe and Janssen 1997). One set relates the free energy of the mixture, the stress and the electrochemical potential to its composition and its deformation (Huyghe et al. 2003). The other relates fluxes to gradients in electrochemical potentials. All of these parameters are generally found to be dependent on orientation and position within the disc (Houben et al. 1997), spinal level, age and species. This paper explores an experimental method to study couplings associated with canine annulus fibrosus tissue chemomechanics. We present three pilot experiments, each of them including relaxation, swelling and shrinking. While in an earlier paper (Huyghe and Drost 2004), we restricted our attention to uniaxial experiments, the present paper reports biaxial experiments only.

Selected paper presented at the IUTAM Symposium on Swelling and Shrinking of Porous Materials: From Colloid Science to Poromechanics – August 06-10 2007, LNCC/MCT.
E-mail: j.m.r.huyghe@tue.nl

METHODS

Lower lumbar motion segments were cut from spines of 2 mongrel dogs and stored at −65 degrees centigrade. One of the vertebral bodies of a motion segment was sawed away almost completely, so that at most a thin layer of bone remained on the top of the intervertebral discs. The posterior half of the segment (arch) was sawed away. The anterior part of the motion segment was allowed to thaw. The surrounding muscle and fat tissues were removed with a scalpel. The nucleus pulposus was carefully removed. During this process, the disc was kept moist by dripping with a physiological salt solution. Lamellae at the anterior part of the annulus fibrosus of at least 10 mm length and a minimal number of branches were selected under the stereo microscope. Lamellae were separated by blunt dissection. Finally, a sample of 10 mm (circumferentially) by 2 to 8 mm (axially) is cut. The thickness of the lamellae was inhomogenous and variable, about 1 mm. The anterior side of each sample was glued upon a flexible polystyrene frame of 15 to 18 mm (Fig. 1) using cyanoacrylate glue (Hyloglue M-100). The frame was cut diagonally to create 4 lips at the 4 sides of the sample, 2 of 15 mm width and 2 other of 18 mm. Traction exerted on 2 opposite 15 mm lips resulted in an extension of the samples along their long axis, i.e. the circumferential direction in the disc. Traction exerted on 2 opposite 18 mm lips resulted in extension of the samples along their short axis, i.e. in the axial direction in the disc. The long axis of the sample had an angle of approximately 30 degrees with the collagen fiber direction. The thickness of the polystyrene lips was 0.5 mm. 3 samples (Table I) were stored at −65 degrees centigrade until use.

A sample was taken out of the freezer, allowed to thaw and, after about 15 minutes, mounted into a horizontal mechanical drawing bench by clamping the polystyrene lips. The 15 mm lips were gripped in 2 opposite clamps moving in the x-direction, and the 18 mm lips were gripped in 2 opposite clamps moving in the y-direction. The procedure is based upon the work of (Myers et al. 1984), (Akizuki et al. 1986) and (Huyghe and Drost 2004). The displacement of 2 x-clamps of the drawing bench was computer controlled. The tensile forces in x- and y-directions were measured by means of 2 force transducers. Above the samples, 2 dripping devices were mounted, one filled with distilled water, and the other filled with a physiological salt solution. The external salt concentration and the clamp position were changed in a stepwise fashion.

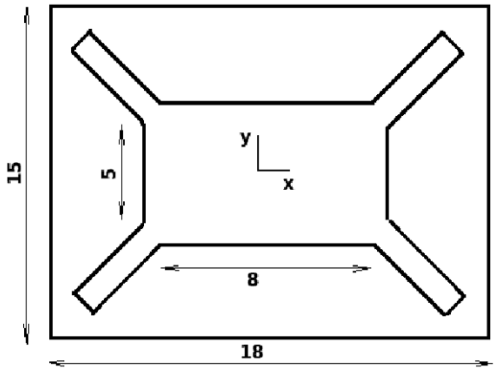

Fig. 1 – Geometry of the polystyrene frame that is used to fix the samples into the biaxial drawing bench. The x-direction coincides with the circumferental direction of the annulus fibrosus sample.

RESULTS

The force tracings associated with three different samples are shown in Figures 2-5. The experimental measurement on the first sample is reported in 2 different figures (Experiment A in Fig. 2, and experiment B in Fig. 3) that report measurement of force in intervals of time separated by half an hour of rest. The thickness of sample 1 is less than 1 mm. The width is about 8 mm. The sample is taken halfway of the outer edge of the annulus fibrosus and the nucleus-annulus interface. The clamp speed at which the step in the strain is applied is 0.05 mm/s. This is sufficiently fast compared to the time constant of the observed phenomena, and sufficiently slow to avoid inertia of the device to come into play. In experiment A, a −12% step in the y-strain is applied at $t = 0$, and a +6% step at $t = 10$ min. A +3% step in the x-strain is applied at $t = 15$ min. The external salt concentration is physiological except between $t = 20$ min and $t = 25$ min, where it is zero. The step in y-strain results in a sharp increase in y-force and a much weaker response of the x-force. The step in the x-strain results in a sharp increase of x-force and a much weaker response of y-force. The responses to salt concentration changes are mild. During the 30 min break, the clamp positions in both x- and y-directions

TABLE I
Samples tested in the biaxial testing device.

sample number	thickness (mm)	origin	force tracings
1	$1 \geq \Delta z$	center annulus	Figs. 2 and 3
2	$\Delta z \approx 1$	outer annulus	Fig. 4
3	$1.1 \geq \Delta z \geq 1$	outer annulus	Fig. 5

have been untouched. At $t = 60$ min, a stepwise increase in x-strain of 6% starts the experiment B (Fig. 3). The y-clamps are immobile during the experiment B. At $t = 120$ min, the x-strain is increased by 6%. The external salt concentration is physiological, except during the periods between $t = 80$ min and $t = 100$ min and between 140 min and 160 min in which the concentration is zero. The contact with distilled water results in an increase of the forces in absolute values (Fig. 3). The experimental measurement of forces on sample 2 are shown in Figure 4, while those associated with sample 3 are shown in Figure 5. The applied boundary conditions are found in the respective captions of the figures. In Figure 4, the x-force has a minor response on changes in salt concentration and a mayor response on the imposed steps of x-strain, while the y-force does the opposite. The y-force responds to a decrease in salt concentration from physiological to zero by a forceful move towards compressive scales. All of the samples exhibit relaxation behavior which continues long after changes in external bath concentrations and strain.

DISCUSSION

The force tracings show strong time, salt concentration and orientation-dependent stresses. The force tracing signature of a response to a change in strain, is one of a jump in stress that relaxes partly as the new strain is maintained. The force tracing signature of a stepwise change in salt concentration is a progressive monotonous change in stress towards a new equilibrium value. When the external concentration c_{ext} of NaCl is reduced from 0.15 M to 0 M, the result is an immediate decrease in external osmotic pressure $\pi = 2RTc_{ext}$. Hence, a steep gradient of the water chemical potential and electrochemical potentials of the ions develops between the tissue and the solution. These gradients induce an influx of water into the tissue and an outflux of ions from the tissue. Volume-wise the outflux of ions is negligible compared to the influx of water. The latter influx of water results in a change in clamp force with time. The time constant associated with the change in salt concentration is typically longer than the time constant associated with the step changes in strain. The response to the changes in strain represent a minimal adjustment of the ionic concentrations, and a major redistribution of the fluid between the sample and the external salt solution. However, the response to a change in salt concentration represents a major redistribution of both the salt and the fluid. The time constant Δt associated with this fluid movement is typically

$$\Delta t = \frac{(\Delta z)^2}{KH} \tag{1}$$

while the time constant for the redistribution of the salt is

$$\Delta t = \frac{(\Delta z)^2}{D} \tag{2}$$

if we assume a negligible convection. In Eqs. (1-2), K is the hydraulic permeability, H the transverse aggregate modulus of the sample, D the diffusion coefficient of the salt, and Δz is the thickness of the sample. The results seem to indicate that the redistribution of the salt takes more time than the fluid redistribution:

$$KH \geq D \tag{3}$$

Even if KH is in the same order as D, convection should slow down a response to a salt concentration, because the salt and the water typically run in opposite directions following a change in salt concentration. Whether a difference of diffusion speed or convection is the reason for the slower response to the salt concentration change is a dilemma to be addressed in future research. The change in strain in one direction is usually accompanied by changes in stress in both directions. Similarly, a change in salt concentration results in

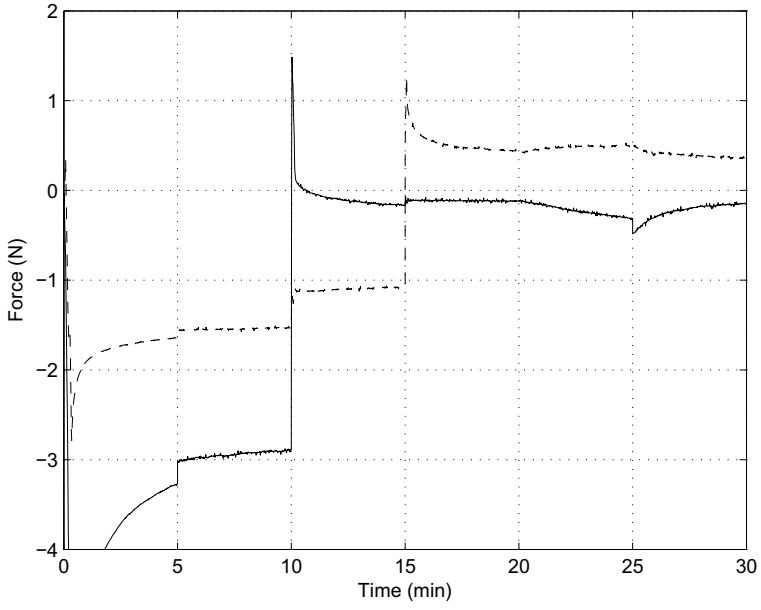

Fig. 2 – x-force recording (discontinuous line) and y-force recording (continuous line) as a function of time in experiment A of sample 1. The thickness of the sample is less than 1 mm. The width is about 8 mm. A -12% step in the y-strain is applied at $t = 0$ and a $+6\%$ step at $t = 10$ min. A $+3\%$ step in the x-strain is applied at $t = 15$ min. The external salt concentration is physiological, except between $t = 20$ min and $t = 25$ min where the concentration is zero. The sample is taken halfway the outer edge of the annulus fibrosus and the nucleus-annulus interface.

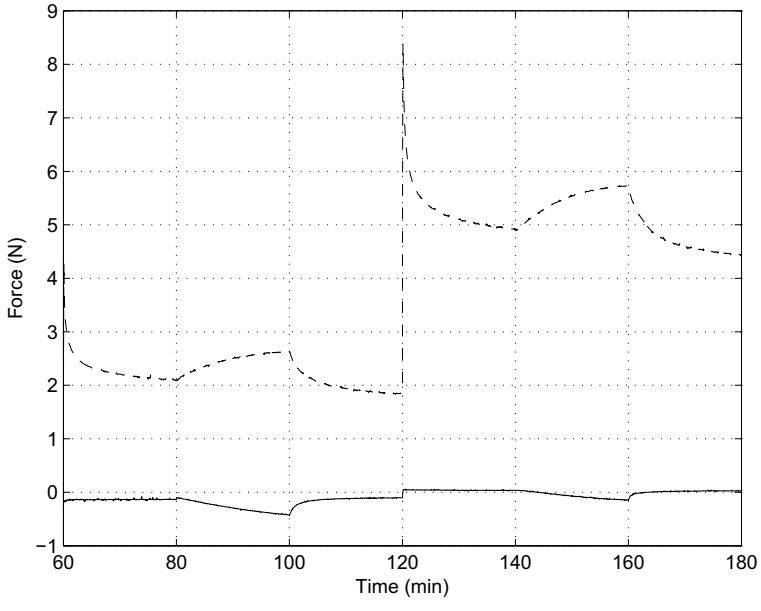

Fig. 3 – x-force recording (discontinuous line) and y-force recording (continuous line) as a function of time in experiment B of sample 1. This experiment is the continuation of experiment A of sample 1 (Fig. 2) after a 30 min interruption of the force measurement. During the break, the clamp positions in both x- and y-directions have been untouched. At $t = 60$ min, a stepwise increase in x-strain of 6% is applied. The y-clamps are immobile during the whole experiment. At $t = 120$ min, a second stepwise increase in x-strain of 6% is applied. The external salt concentration is physiological, except during the periods between $t = 80$ min and $t = 100$ min, and between 140 min and 160 min in which the concentration is zero.

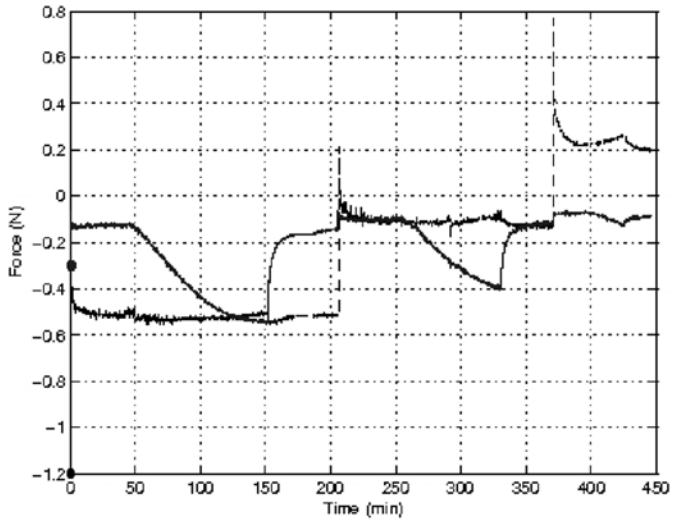

Fig. 4 – Clamp force recordings in x-direction (black) and clamp force recordings in y-direction (blue) as a function of time in experiment 2. A solid black dot along the force scale indicates the force level at $t = 0$ for the x-tracing. A solid blue dot along the force scale indicates the force level at $t = 0$ for the y-trace. A 3% step in the strain is applied at $t = 205$ min, and an additional 6% step in the strain at $t = 375$ min in the x-direction. The strain in the y-direction is constant throughout the experiment.The external salt concentration is physiological, except in the periods between $t = 50$ min and $t = 150$ min, between $t = 255$ min and $t = 330$ min, and in the period $t = 400$ min and 430 min in which the external salt concentration is zero. The thickness of the sample is about 1 mm. The sample is taken from the outer annulus region. The clamp speed at which the step in the x-strains is applied is 0.05 mm/s.

a readjustment of stress in both directions, being it in different measures. Although the small number of samples does not allow any definitive quantitative conclusions, the trends shown in the tracings may shed light on the complex interaction between the directionality of forces, strains and fiber orientation on the one hand and on the osmolarity of the tissue on the other hand. The dual response to a stepwise change in strain is understood as an immediate response before fluid flows in or out of the tissue, followed by a progressive readjustment of the fluid content in time because of the gradient in fluid chemical potential between the tissue and the surrounding solution. The sensitivity to changes in salt concentration can be qualitatively understood in the context of chemoelectromechanical theory (Huyghe and Janssen 1997).

In Figure 4, the x-force has a minor response to changes in salt concentration, and a major response to the imposed steps of x-strain, while the y-force does the opposite. The behavior can be understood as the response of a sample in which the fibers are primarily oriented parallel to the x-axis. Indeed, the y-response is dominated by the proteoglycan gel swelling and shrinking under changing salt concentration, while the x-response is sensitive to strains because of the stiffness of the fibers.

Unlike in Figure 4, the responses in Figure 5 of both force tracings to changes in x-strain and salt concentrations are similar.

The response of the x-force to changes in x-strain, however, is more forceful than the corresponding response of the y-force. The response of the y-force to changes in salt concentrations is more pronounced than the corresponding response of the x-force. This result seems to indicate a more isotropic and cross-linked distribution of fibers in the sample 3 compared to sample 2. Elastic stiffness, as computed from these experiments, is rather inaccurate, because of ill-defined cross-sectional areas and specimen to specimen variability. The elastic stiffness is between 10 and 20 MPa , and is definitely higher than the stiffnesses computed from uniaxial experiments (Galanta 1967, Huyghe and Drost 2004) which in turn are somewhat higher than typical values of confined compression tests (Houben et al. 1997, Huyghe et al. 2003). The higher stiffnesses observed in tensile versus compressive experiments are observed in articular cartilage as well (Stoltz and Ateshian 2000).

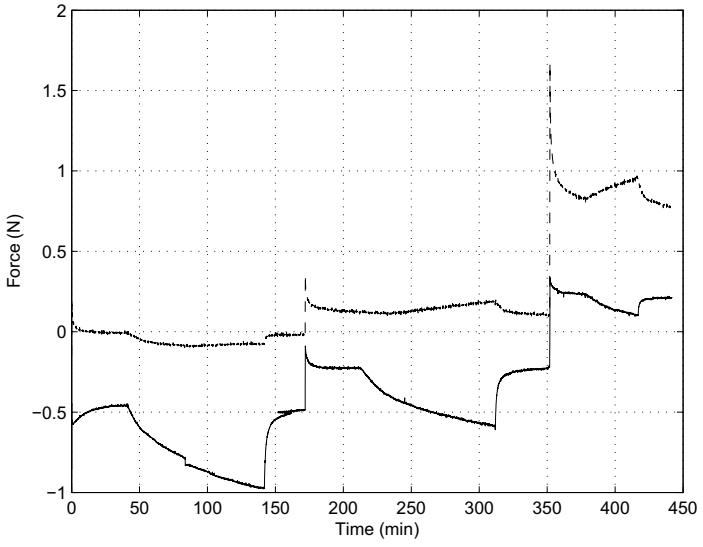

Fig. 5 – Recording of x-force (upper tracing) and y-force (lower tracing) as a function of time in experiment 3. At $t = 170$ min, a step in the x-strain of 3% is imposed, and at $t = 350$ min an additional step of 6% is imposed. The y-strain is constant. The external salt concentration is physiological except in the periods between $t = 40$ min and $t = 145$ min, between $t = 210$ min and $t = 320$ min, and in the period $t = 380$ min and 410 min in which the external salt concentration is zero. The thickness of the sample is between 1 mm and 1.1 mm. The sample is taken from the outer annulus fibrosus of the same disc as the sample of experiment 2 of Huyghe and Drost (2004). The clamp speed at which the step in the x-strain is applied is 0.05 mm/s.

ACKNOWLEDGMENTS

The author gratefully acknowledge the support of W. Meertens and M. van Hout for preparing the samples and performing the experiments, and M. Drost for his advise. This research is part of the project GENODISC (Call identifier: FP7-HEALTH-2007-A, Project number 201626), funded by the European Union.

RESUMO

A mecânica in vivo do anel fibroso do disco intervertebral é baseada em carregamento biaxial ao invés de uniaxial. As propriedades materiais do anel estão intimamente ligadas à osmolaridade no tecido. O artigo apresenta experimentos de relaxação biaxiais do anel fibroso de um tecido canino sob mudanças abruptas na concentração externa de sal. A assinatura da força devido à mudança brusca de salinidade resulta em uma progressiva e monótona mudança na tensão em direção a um novo valor de equilíbrio. Embora o número de amostras não permita nenhuma conclusão quantitativa, as tendências podem abrir uma luz no entendimento das interações complexas na direção das forças, deformações e orientação das fibras por um lado e a osmolaridade do tecido por outro lado. A resposta dual devido à uma mudança na deformação é compreendida como uma resposta imediata antes do fluido escoar para dentro ou para fora do tecido, seguido de uma progressiva readaptação da quantidade de fluido no tempo devido ao gradiente do potencial químico entre o tecido e a solução externa.

Palavras-chave: inchamento, colágeno, osmose, Donnan, tecido cartilaginoso.

REFERENCES

AKIZUKI S, MOW VC, MUELLER F, PITA JC, HOWELL DS AND MANICOURT DH. 1986. Tensile properties of human knee joint cartilage: I. Influense of ionic conditions, weight bearing, and fibrillation on the tensile modulus. JOR 4: 379–392.

GALANTA JO. 1967. Tensile properties of the human lumbar annulus fibrosus. Acta Orthop Scan Suppl 100(1): 5–91.

HOUBEN GB, DROST MR, HUYGHE JM, JANSSEN JD AND HUSON A. 1997. Non-homogeneous permeability of canine annulus fibrosus. Spine 22: 7–16.

HUYGHE JM. 1999. Intra-extrafibrillar mixture formulation of soft charged hydrated tissues. J Theor Appl Mech 37(3): 519–536.

HUYGHE JM AND DROST MR. 2004. Uniaxial tensile testing of canine annulus fibrosus tissue under changing salt concentrations. Biorheology 41: 255–261.

HUYGHE JM AND JANSSEN JD. 1997. Quadriphasic mechanics of swelling incompressible porous media. Int J Eng Sci 35: 793–802.

HUYGHE JM, HOUBEN GB, DROST MR AND VAN DONKELAAR CC. 2003. An ionised/non-ionised dual porosity model of intervertebral disc tissue: experimental quantification of parameters. Biomech Model Mechan 2: 3–19.

IATRIDIS JC, LAIBLE JP AND KRAG MH. 2003. Influence of fixed charge density magnitude and distribution on the intervertebral disc: applications of a poroelastic and chemical electric (peace) model. ASME J Biomech Eng 125: 12–24.

MYERS ER, LAI WM AND MOW VC. 1984. A continuum theory and an experiment for the ion-induced swelling behavior of articular cartilage. ASME J Biomech Eng 106(2): 151–158.

SCHROEDER Y, ELLIOT SJ, WILSON W, BAAIJENS FPT AND HUYGHE JM. 2008. Experimental and model determination of human intervertebral disc osmoviscoelasticity. J Orthoped Res 26: 1141–1146.

SCHROEDER Y, WILSON W, HUYGHE JM, MAROUDAS A AND BAAIJENS FPT. 2006. Osmoviscoelastic finite element model of the intervertebral disc. Eur Spine J 15: 361–371.

STOLTZ MA AND ATESHIAN GA. 2000. A conwise linear elasticity model for the analysis of tension-compression non-linearly in articular cartilage. ASME J Biomech Eng 122: 576–586.

VAN LOON R, HUYGHE JM, WIJLAARS MW AND BAAIJENS FPT. 2003. 3d fe implementation of an incompressible quadriphasic mixture model. Int J Numer Meth Engng 57: 1243–1258.